HNPS Advances in Nuclear Physics

Vol 19 (2011)

HNPS2011

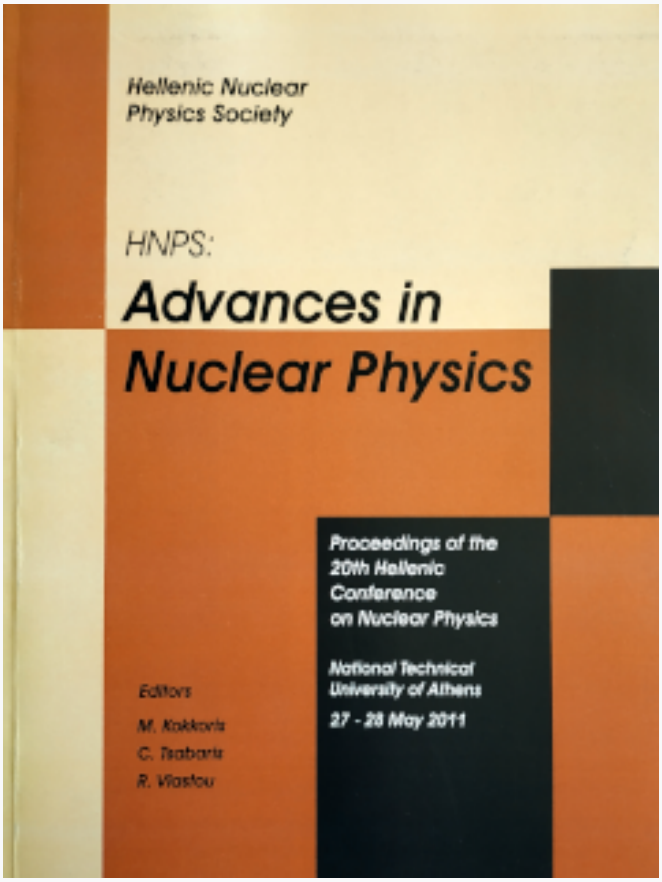

Inelastic cross sections in relativistic deuterons on Lead reactions

M. Zamani, S. Stoulos, M. Fragopoulou, M. Krivopustov

doi: 10.12681/hnps.2520

Inelastic cross sections in relativistic deuterons on Lead reactions

M. Zamani[1*], S. Stoulos[1], M. Fragopoulou[1] and M. Krivopustov[2]

[1] *Aristotle University of Thessaloniki, School of Physics, Thessaloniki 54 124, Greece*
[2] *Joint Institute for Nuclear Research (JINR) Dubna, 141980, Russia*

Abstract
The inelastic cross section of deuterons hitting a Lead target has been determined by the beam attenuation technique. A spallation neutron source based on Lead target has been irradiated with 1.6 and 2.5 GeV deuterons. Solid state nuclear track detectors as well as the activation method were used in order to obtain the neutron and proton distribution along the surface of the source. The attenuation coefficient was estimated by fitting the experimental data taking into account the build up effect and the beam attenuation. Using the attenuation coefficient, the interaction length and then the inelastic cross section of deuterons on Lead reaction have been determined.

Keywords: Spallation reactions, deuteron induced reaction, inelastic cross section.

1. Introduction

The applications of AD Systems in Nuclear Waste Incineration [1] and Energy Production [2] require a precise prediction of the energy spectrum and the angular distribution produced by a spallation target. In the majority of the experiments and calculations, the accelerator bombards a heavy target with high energy light particles, mainly protons [3-8]. Such experiments have been performed in Dubna, using a large cylindrical Lead target, surrounded by a U-blanket [9-11]. The efficiency of a spallation source depends critically on the average number of neutrons produced per primary proton in the target material. This number can be increased by using higher proton energies or particles heavier than protons. A large number of experiments were also performed by deuterons, alphas, carbon, etc. [12-14]. In most cases, calculations describe well the experimental data, although the accuracy of existing spallation models used to estimate neutron and proton spatial distributions and in residual production cross sections is still far from the performance required for technical applications [15, 16]. The discrepancy between the experimental data and the model calculations can be attributed to the accuracy of the cross sections measurements, which must be lower than 5% [17]. Another reason is that some cross sections are not available in databases.

[*] Corresponding author. Postal address: Aristotle University of Thessaloniki, School of Physics, Thessaloniki 54 124, Greece, Tel: +302310998176, Fax: +302310998176
E-mail address: zamani@physics.auth.gr

Deuteron beams are the second best option after protons for calculations and experiments. The analysis of deuteron induced reactions is a difficult task, since deuteron is a weakly bound composite system, which easily undergoes break up reactions. To deal with this problem, several methods of calculations have been developed. The reported cross section calculations of deuteron reactions on heavy targets, used as spallation targets, such as ^{232}Th, ^{209}Bi, $^{235/8}$U and $^{206\text{-}8}$Pb, are mostly referred to low energies, considerably lower than the ones required for transmutation experiments [18-22]. Limited experimental results have been published on high energy deuteron reaction cross sections on heavy targets [12-13, 23-25]. By side measurements, taken at angles near 90^{o}, the inelastic cross section is essentially subtracted from the total cross section and therefore, the inelastic cross section can be determined with high accuracy. In the present work, these kinds of experiments have been carried out at the Nuclotron accelerator of the High Energy Laboratory of Joint Institute of Nuclear Research (JINR) in Dubna, Russia. The inelastic cross sections of high energy deuterons on Lead target have been determined by using the attenuation technique.

2. Experimental

The experimental set-up, called "Energy plus Transmutation", consists of a Lead target, 50 cm in length and 8 cm in diameter, surrounded by a natural Uranium blanket. Four sections of the target constituted the spallation source. Each section has been covered by 30 U-rods, which is the blanket. Each rod had a cylindrical form, with 10.4 cm in length and 3.6 cm in diameter. The whole system was surrounded, for radiation protection reasons, by a polyethylene moderator, covered by Cd of 1 mm thickness [9]. The Lead target has been irradiated by 1.6 and 2.5 GeV deuterons, mostly producing intermediate and fast neutrons [11, 25].

Escaping neutron distributions were studied along the U-blanket surface, parallel to the target axis, which is also the beam axis. This sample arrangement corresponds to neutron and proton emissions at large angles relative to the beam direction. Solid State Nuclear Track Detectors (SSNTDs) and activation detectors have been used for the measurement of neutron and proton spatial distribution. SSNTDs are not sensitive to gamma rays and detect particles with high efficiency.

In this work, CR39 foils (Pershore Mouldings) were used as alpha particle detectors. One part of the detectors was in contact with a neutron converter (Kodak

LR115 type 2B, containing $Li_2B_4O_7$). This converter provides information about the neutron fluence of all energies, detecting the tracks of alpha particles, emitted by $^{10}B(n,\alpha)^7Li$ and $^6Li(n,\alpha)^3H$ reactions and registered on the CR39 detector. One part of CR39, which was in contact with the converter, was covered on both sides with 1 mm Cd foils, thus detecting epithermal and fast neutrons. The thermal neutron component (up to 1 eV) was calculated by subtracting the measured alpha particle density of the Cd-covered from the Cd-uncovered region of the CR39 detector. Fast neutrons were also measured by proton recoil tracks on the detector itself, deriving from the neutron elastic scattering on the H of the detector). The neutron energy region detected by proton recoils is between 0.3 and 3 MeV, due to limitations in proton registration efficiency [26]. Fast neutrons above 2 MeV were measured via Th-232 fissions on a Lexan detector. For this purpose 300 μg Th-232 were evaporated on the Lexan surface.

The neutron distribution along the U-blanket surface was also determined by using activation detectors. Depleted U ($^{235}U/^{238}U = 0.18 \pm 0.01\%$), natural Au samples (mass ~3 up to 6 mg, thickness ~1 μm) and natural Cd foils (mass ~ 2g, purity 99.9%, thickness 1 mm) have been used as activation detectors. ^{nat}Cd effectively captures neutrons below 1 eV, due to the high capture cross section of ^{113}Cd to thermal-epithermal neutrons, while it can be used as well for neutron detection above 1 eV, via the $^{114}Cd(n,\gamma)^{115}Cd$ reaction. Moreover, ^{nat}Cd has a significant cross section to $^{nat}Cd(p,x)^{111}In$ reaction, in the energy range of $1\ MeV \leq E_p \leq 400\ MeV$, responding well to the emitted proton spectrum [27]. Corrections were applied for proton energy reduction, as well as for neutron self-absorption, due to the foil thickness [28].

3. Results and Discussion

Secondary neutrons and fewer protons are the main particles created in an interaction of light particles with heavy targets. The neutron spectrum contains a hard part, corresponding to nuclear cascade effects, which take place in the target. The neutron spectrum is theoretically extended up to the deuteron beam energy. Practically, secondary neutron energies reach approximately the half of the incident energy. Another neutron component, superimposed on the fast neutron spectrum, dominates the low energy part, peaking at energies around 1 MeV. The low energy neutron spectrum can be attributed to light particle evaporation from highly exited

target nuclei during the intranuclear cascade reaction stage. Neutrons having energies above 1 MeV induce uranium fission that becomes a secondary source of neutrons. By this target arrangement, a multiplication of Lead target emitted neutrons takes place. Secondary protons produced at the stage of deuteron interaction with the Lead target, can also induce uranium fissions through (p,f) reactions, although (p,f) cross sections become important for proton energies above 60-100 MeV. The spectrum of the escaped neutron peaks at 0.7-0.8 MeV, as it was calculated [29, 30] and also confirmed experimentally during these experiments [31]. Protons escaping the U-blanket surface derive from direct interactions of high energy neutrons and protons produced by the target and induce further reactions at the Uranium mass, during the internuclear cascade stage.

The spatial neutron distribution along the U-blanket surface, normalized to the beam intensity, is presented in Figure 1, for 1.6 GeV deuterons. The neutron energy ranges have been taken by different detectors that have good response in the given neutron energy intervals, as indicated in the figure. All curves, although they correspond to different neutron energy ranges, can be used for the determination of the beam attenuation coefficient in Lead.

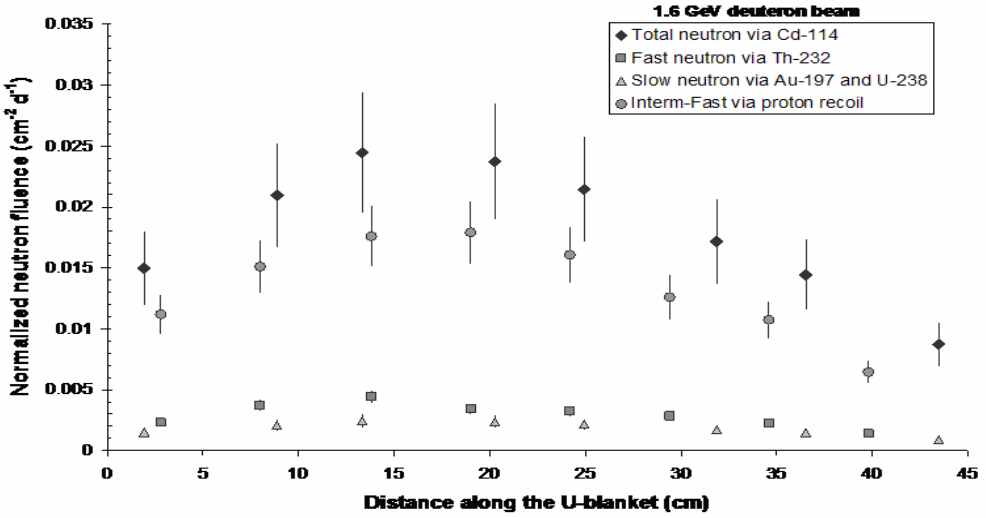

Fig.1. Spatial neutron distribution normalized to the beam intensity along the target surface, for various neutron energy ranges obtained during irradiation by 1.6 GeV deuteron beam energy on Lead target.

In Figure 2, the normalized total neutron fluence is presented for both deuteron energies applied in the experiment. A similar spatial distribution can be observed for both deuteron energies, with a small peak coming arising from the combination of a build-up effect at the beam entrance and the beam attenuation. The built up zone is usually observed at the target head due to the internuclear cascade. The second part of the curve corresponds to the exponential decrease of the beam along the target axis. However, the role of ionization loss, pair production and other effects, play an important role in the beam attenuation, mainly for secondary particles with energies ≤100 MeV [27]. Indeed, as the energy of secondary particles has a mean value of 120 MeV for a beam with energy around 1 GeV and the ternary particles' mean energy is 60 MeV [32], the beam attenuation can be easily understood. The normalized proton distributions measured at the U-blanket surface are given in Figure 3. The shape of the neutron and proton spatial distribution measured along the U-blanket surface can be described satisfactory by the above physics.

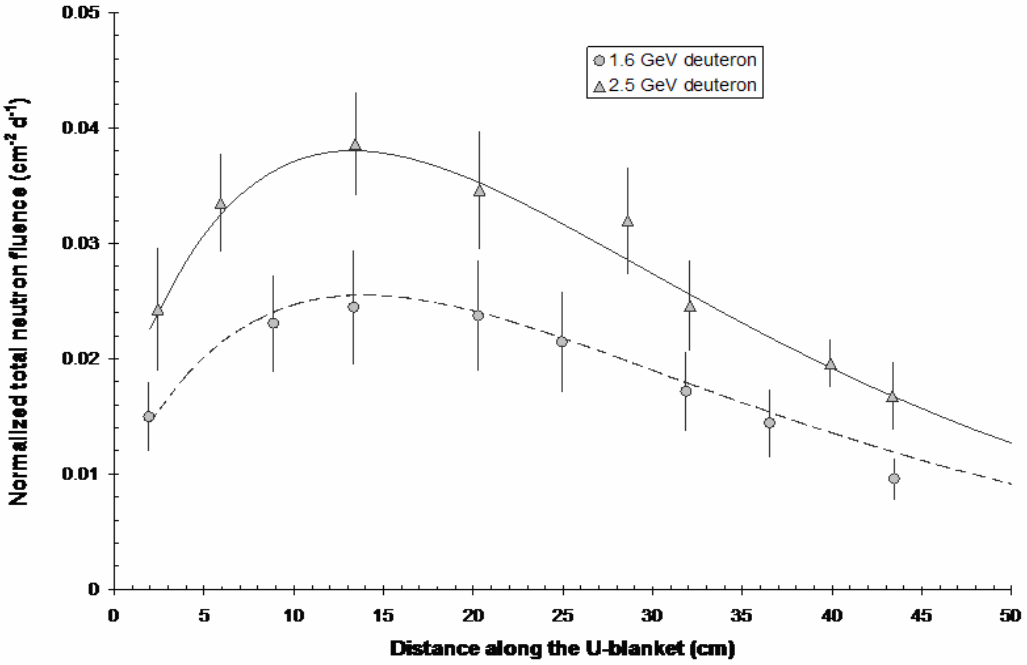

Fig.2. Spatial neutron distributions normalized to the beam intensity along the target surface, for various incoming deuteron beam energies. The lines refer to the fitting process using Equation (1).

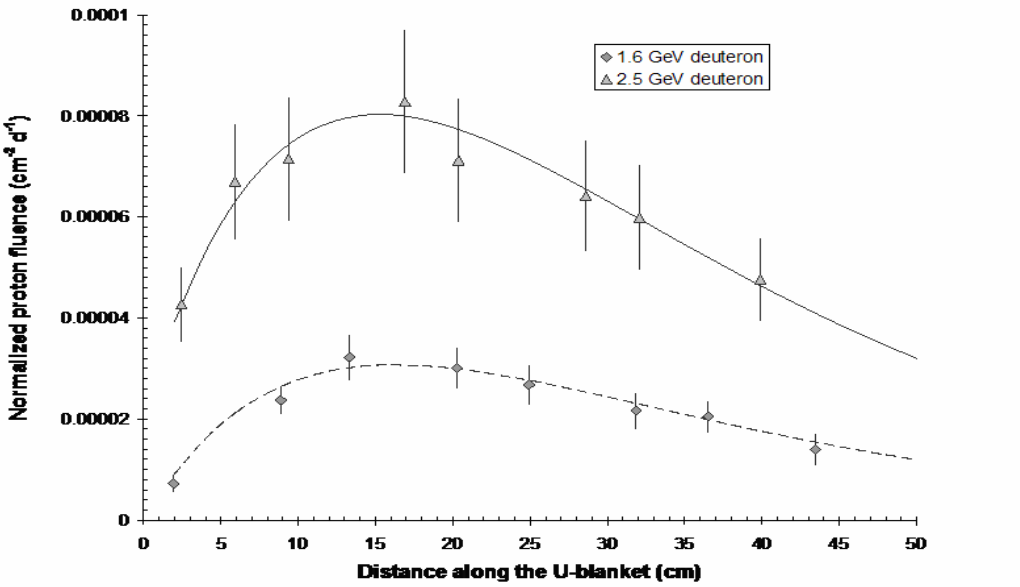

Fig.3. Spatial proton distributions normalized to the beam intensity along the target surface, for various incoming deuteron beam energies. The lines refer to the fitting process using Equation (1).

A fitting procedure has been applied to the total neutron fluencies per incident deuteron (ρ_n, n cm^{-2} deuteron^{-1}) measured over the U-blanket surface, taking into account the above discussion. The following equation was used:

$$\rho_n = C\,(1-ae^{-bx})\,e^{-dx} \qquad (1)$$

where C is a parameter in units neutrons cm^{-2} deuteron^{-1}. The first part of the equation was set to describe the build up effect with the build up parameter **a** and the build up coefficient **b**. The second part represents the beam attenuation along the target as it was observed over the moderator surface with the attenuation coefficient d (cm^{-1}). The attenuation coefficient d is related to the interaction length λ of the primary deuterons in Lead by $d=1/\lambda$. Using the determined interaction length, the inelastic cross section of deuterons in Lead can be estimated by the relationship between the interaction length and the inelastic cross section by $\sigma = A/N\lambda\rho$. A is the Lead atomic number, N is the Avogadro's number and ρ is the Lead target density (gr cm^{-3}) [32].

The parameters deduced from the fitting of the distribution curves are given in Tables 1 and 2, for 1.6 and 2.5 GeV deuterons respectively. In the tables, a remarkable agreement must be noted for all parameters deduced by the fitting, independently of the method of the measurement applied. These parameters depend on the target geometry and neutron energy range, especially when they are used to

describe hadrons leakage distribution on the surface of the target [27] or on the surface of the spallation target, as it is the case of the presented experiment. Practically, the interaction cross section can be estimated by the attenuation observed by the intermediate – fast neutrons representing the majority of the neutron spectrum on the U-blanket surface as it can be seen in Figure 1.

Table 1. Calculated fitting parameters and inelastic cross section estimated for deuteron 2.5 GeV in Pb target.

Fitting parameters	**Fast neutron**	**Total neutron**	**Total proton**
Parameter C (cm^{-2} d^{-1})	0.024 ±0.002	0.48 ±0.06	0.0021 ±0.0002
Build-up parameter a	1.00 ±0.02	0.97 ±0.02	0.99 ±0.02
Build-up coefficient b (cm^{-1})	0.013 ±0.004	0.011 ±0.005	0.005 ±0.002
Attenuation coefficient d (cm^{-1})	0.054 ±0.006	0.057 ±0.005	0.054 ±0.006
Inelastic cross section (b)	**1.65 ±0.18**	**1.73 ±0.15**	**1.65 ±0.18**

Table 2. Calculated fitting parameters and inelastic cross section estimated for deuteron 1.6 GeV in Pb target.

Fitting parameters	**Fast neutron**	**Total neutron**	**Total proton**
Parameter C (cm^{-2} d^{-1})	0.045 ±0.006	0.31 ±0.05	0.00053 ±0.00006
Build-up parameter a	0.97 ±0.02	0.97 ±0.02	1.00 ±0.02
Build-up coefficient b (cm^{-1})	0.014 ±0.006	0.012 ±0.006	0.009 ±0.007
Attenuation coefficient d (cm^{-1})	0.059 ±0.006	0.055 ±0.006	0.057 ±0.007
Inelastic cross section (b)	**1.79 ±0.18**	**1.66 ±0.18**	**1.72 ±0.21**

The inelastic cross sections deduced by this experiment are also presented in Tables 1 and 2 for the two energies studied. A mean value from the three measurements leads to 1.68 ± 0.17 and 1.73 ± 0.19 barns for 2.5 and 1.6 GeV deuterons respectively on Lead target. We refer to inelastic cross sections, instead of total cross sections, because the neutron and proton distributions, measured at the U-blanket surface, correspond to particles escaping at large angles (around 90^o) relative to the beam and therefore, events from elastic scattering are not included in these measurements. In both cases, deuteron inelastic cross sections are very close to those found when the same target is irradiated with protons of the same energy [3, 6, 7]. A similar result can be concluded by V.S. Barashenkov calculations and experimental data [18].

A simple calculation based on the geometrical cross sections:

$$\sigma = \pi r_o^2 \left(A_p^{1/3} + A_T^{1/3} - \beta \right)^2 \qquad (2)$$

give a σ of 2.4 barns for the total reaction cross section. In Equation (2), A_p and A_T indicate the projectile and the target mass respectively; r_o was taken 1.48 fm and β

1.32 [33]. However, this value is slightly higher than the one determined in this experiment, due to the fact that the elastic cross section value is also included.

Figure 4 presents the experimental data available in literature for proton as well as neutron cross sections, corresponding to the same energies.

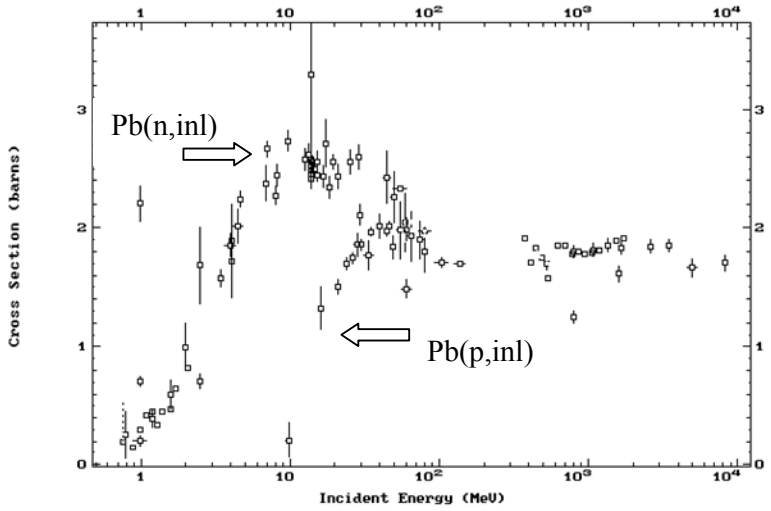

Fig.4. Inelastic cross section data of relativistic proton and neutron induced reaction in Lead.

The deuterons inelastic cross sections, as it was deduced from this experiment, are also compatible with neutron and proton cross section data at the same energy region with deuterons' beam energy.

4. Conclusion

The inelastic cross section of deuteron interactions with Lead has been determined by the beam attenuation technique. The attenuation coefficient derived by applying a fitting procedure to the spatial neutron distribution measured along the surface of a massive spallation neutron source, consisted of Lead target, surrounded by a ^{nat}U-blanket.

Cross sections of 1.68 ± 0.17 and 1.73 ± 0.19 barns were determined for 2.5 and 1.6 GeV deuterons respectively on Lead. Inelastic cross sections of this work are very close to those resulted by proton irradiations of the same target at similar energies. However, if we consider that a part of deuteron interactions with Lead corresponds to separate interactions of protons and neutrons due to deuteron break up, we conclude that in effect, proton and neutron cross sections are measured at the same

time. This result is compatible with Anderson's suggestion that both protons and neutrons react with a target [34]. This proposition can be supported by the fact that proton and neutron cross sections have the same value. Indeed, calculations of neutron inelastic cross sections in Lead [35] show that neutron and proton cross sections have an identical behavior at the GeV energies. Moreover, previous measurements give the same result for the corresponding energy range [4, 35, 12]. Early neutron reaction cross sections measured at GeV [36-40] show the same values and can be compared with recent measurements, taking into account that cross sections above 1 GeV have no significant variation.

Acknowledgment
The authors are grateful to Professor A.I. Malakhov and the staff of the Laboratory of High Energies, JINR Dubna, for his continuous support to our work. Special gratitude is due to Professor A.D. Kovalenko and the operation staff of the NUCLOTRON accelerator for providing high intensity beams during irradiations.

References

[1] C. D. Bowman, et al., Nucl. Instr. and Meth. Phys. Res. A 320 (1992) 336
[2] C. Rubbia et al. CERN/AT/95-44, 1995
[3] F.F.Chen, C.P.Leavitt, A. Shapiro, Phys.Rev. 99b (1955) 857
[4] R.E.Pollock and G. Schrank, Phys. Rev. 140 B (1965) 575
[5] D. Hilscher, U. Jahnke, F. Goldenbaum, L. Pienkowski, J. Galin, B. Lott, Nucl. Instr. and Meth. Phys. Res. A 414 (1998) 100
[6] A. Letourneau, et al., Nucl. Instr. and Meth. Phys. Res. B 170 (2000) 299
[7] C-M Herbach et al., Nucl. Instr. And Meth. Phys. Res. A 562 (2006). 729
[8] J.M. Carpenter, T. A. Gabriel, E. B. Iverson, D. W. Jerng, Physica B 270 (1999) 272
[9] M.I. Krivopustov, et al., Kerntechnik 68 (2003) 48
[10] M. Zamani, M. Fragopoulou, S.Stoulos, M.I.Krivopustov, A.N.Sosnin, R.Brandt, W.Westmeier, M. Manolopoulou, Rad. Measurements 43, S1 (2008) 51
[11] S. Stoulos, M. Fragopoulou, A. Sosnin, M. Manolopoulou, M. Krivopustov, M. Zamani, Nucl. Instr. and Meth. Phys. Res. A 599 (2009) 106
[12] B. Lott, F. Cnigniet, J. Galin, F. Goldenbaum, D. Hilscher, A. Liénard, A. Péghaire, Y.Périer, X. Qian, Nucl. Instrum. and Meth. Phys. Res. A 414 (1998) 117
[13] L. Pienkowski, F. Goldenbaum, D. Hilscher, U. Jahnke, J. Galin, B. Lott, Phys. Rev. C 56 (1997) 1909
[14] R.Brandt et al., Rad. Measurements 43, S (2008) 132
[15] J. Cugnon, C. Volant and S.Vuillier, Nucl. Phys. A 625 (1997) 729
[16] S. Leray, et al., Phys. Rev. C 65 (2002) 044621
[17] V. Artisyuk, C. Broeders, E. Gonzalez-Romero, W. Gudowski, A. Ignatyuk, A.Konobeyev, Yu Korovin, G. Pilnov, A. Stankovskiy, Yu Titarenko, Progress in Nuclear Energy 50 (2008) 341
[18] V.S. Barashenkov, V.D. Toneev, S.E.Chigrinov, 1975, Plenum Publishing Corporation (Translated from Atomnaya Energiya, 37 (1974) 480
[19] P. Chau Huu-Tai, Nucl. Phys. A 773 (2006) 56
[20] F.Ditroi, F. Tarkanyi, S.Takacs, M.S.Uddin, M.Hagiwara, M.Baba, A.Ignatyuk, S.F.Kovalev, Journ. Radioanalytical and Nucl. Chem. 276 (2008) 835

[21] H.Buyukuslu, A. Kaplan, E.Tel, A. Aydin, G. Yildirim, M.H.Bolukdemir, Annals of Nucl. Energy, 37 (2010) 534
[22] D.Ridikas, W.Mittig, H.Savojols, P.Roussel-Chomaz. S.V.F¨ortsch, J.J.Lawrie, F.Steyn, Phys.Rev. C 63 (2000) 014610
[23] S.Mayo, W.Schimmerling, M.J.Sametband, Nucl. Phys. 62 (1965) 393
[24] T.Enqvist et al. Nucl. Phys. A 703 (2002) 435
[25] M.I. Krivopustov,, et al., J.Radianal.Nucl.Chem., 279 (2009) 567
[26] J.R. Harvey, R.J. Tanner, W.G. Alberts, D.T. Bartlett, E.K.A. Piesch and H. Schraube, Rad. Prot. Dosim. 77 (1998) 267
[27] G. S. Bauer, Nucl. Instrum. Meth. Phys. Res. A 463 (2001) 505
[28] M. Manolopoulou, S. Stoulos, M. Fragopoulou, R. Brandt, W. Westmeier, M.I. Krivopustov, N.A. Sosnin, S.R. Hashemi-Nezhad, M. Zamani-Valasiadou, Nucl. Instr. and Meth. Phys. Res. A 586, (2008) 239
[29] A. Krása, et al., JINR Preprint E1-2005 (2005) 46
[30] S.R. Hashemi-Nezhad, Igor Zhuk, M. Kievets, M.I. Krivopustov, A.N. Sosnin, W. Westmeier, R. Brandt, Nucl. Instr. Meth. Phys. Res. A 591 (2008) 517
[31] M.Zamani-Valasiadou, M.Fragopoulou, M.Manolopoulou, S.Stoulos, S.Jokic, A.N. Sosnin, M.I. Krivoustov, Ann.Nuclear Energy 37 (2010) 241
[32] A.H.Sullivan, A Guide to Radiation and Radioactivity Levels near High Energy
[33] J.Hufner, Phys Reports 125 (1985) 129
[34] L.Anderson, W.Brückner, E.Moeller, S.Nagamiya, S.Nissen-Meyer, L.Schroeder, G.Shapiro, H. Steiner, Phys. Rev. C 28 (1983) 1224
[35] G.Folger and V. Grichine, EUDET-Memo-2007-18
[36] J.H.Atkinson, W.N. Hess, V.Perez-Mendez, R.W.Wallace, Phys. Rev. Lett. 2 (1959) 168
[37] J.H.Atkinson, W.N. Hess, V.Perez-Mendez, R.W.Wallace, Phys. Rev. 123 (1961) 1850
[38] T.Coor, D.A.Hill, W.F.Hornyak, L.W.Smith, G.Snow, Phys. Rev. 98 (1955) 1369
[39] M.S. Sinha and N.C. Das, Phys.Rev. 105 (1957) 1587
[40] W. Schimmerling, T.J. Devlin, W.W. Johnson, K.G. Vosburght, R. E. Mischkeal, Phys. Rev. C 7 (1973) 248